

Thermodynamic properties of perfluoro-*n*-octane

A.M.A. Dias^a, A.I. Caço^a, J.A.P. Coutinho^a, L.M.N.B.F. Santos^b, M.M. Piñeiro^c,
L.F. Vega^d, M.F. Costa Gomes^e, I.M. Marrucho^{a,*}

^a CICECO, Department of Chemistry, University of Aveiro, 3810-193 Aveiro, Portugal

^b CIQ, Dep. de Química, Faculdade de Ciências da Universidade do Porto, 4169-007 Porto, Portugal

^c Department of Applied Physics, Faculty of Sciences, University of Vigo, E-36200 Vigo, Spain

^d Institut de Ciència de Materials de Barcelona (ICMAB-CSIC), Campus de la UAB, 08193 Bellaterra, Barcelona, Spain

^e Laboratoire de Thermodynamique des Solutions et des Polymères, Université Blaise Pascal, Clermont Ferrand, 63177 Aubière, France

Received 16 January 2004; accepted 2 July 2004

Available online 25 September 2004

Abstract

Fluorocarbons are attracting much attention nowadays because of their unique properties, which may provide interesting applications in areas as wide as environmental, biomedical and material science. However, the behavior of these compounds is not well understood and only scattered data can be found in the open literature and company technical reports.

In this work, three important properties of perfluoro-*n*-octane were experimentally determined: the liquid density, the vapor pressure and the oxygen solubility. Liquid density was measured, in the temperature range between 288 and 313 K with a vibrating tube densimeter and vapor pressure was measured with an apparatus based on the static method up to 333 K.

The solubility of oxygen in perfluoro-*n*-octane, in the temperature range between 288 and 313 K and at pressures close to atmospheric, was determined experimentally with a precision apparatus based on the saturation method at constant pressure. Experimental solubility data, density and vapor pressure were correlated with the soft-SAFT EoS.

© 2004 Elsevier B.V. All rights reserved.

Keywords: Oxygen; Perfluoro-*n*-octane; Solubility; Density; Vapor pressure; Thermodynamic functions; Regular Solution Theory; Soft-SAFT EoS

1. Introduction

Due to their specific and unusual properties, fluorinated molecules such as perfluorocarbons (PFCs) and their derivatives represent a very interesting and stimulating class of chemicals in physical chemistry and polymer sciences. Perfluorochemicals are non-polar highly fluorinated compounds and as a result of the strong intramolecular bonding (C–F bonds are 485 kJ mol⁻¹, that is 84 kJ mol⁻¹ more than a regular C–H bond), they are chemical and biochemical inert. The chemical structure and the weak intermolecular interactions are responsible for the specific properties of PFCs namely low surface tensions (<20 mN m⁻¹), dielectric constants and refractive indices, and high densities, viscosities

and gas solubilities, which are the largest known for liquids [1].

PFCs have been introduced in a wide variety of areas such as surfactants in supercritical solvents, environmental probes, anticorrosive and antifriction components, as flame retardants, water repellents, or sliding agents, in paints, coatings, polymer technology, metal working and uranium recovery process. The most relevant applications are found in the biomedical field: they can be used in tissue oxygenation fluids (blood substitutes, oxygen therapeutics), anti-tumoral agents, perfusates for isolated organs, surgical tools for ophthalmology, lubrication and cushioning for articular disorders, diagnostic imaging agents, cell culture media supplements and drug formulations and delivery.

Several studies performed in a wide range of liquid PFCs for intravascular use, permitted to conclude that the liquid perfluorocarbon must present some particular properties, such as

* Corresponding author. Tel.: +351 234 370200; fax: +351 234 3700.
E-mail address: imarrucho@dq.ua.pt (I.M. Marrucho).

high gas dissolving capacities, an average molecular weight in the range from 420 to 460, a viscosity less than 5 cP at 298.15 K, a density less than 2.0 g cm^{-3} at 298.15 K, a boiling point greater than 328.15 K, a vapor pressure less than 13 kPa at 298.15 K and a surface tension less than 17 mN m^{-1} at 298.15 K [2].

There are very little data in the open literature for these compounds and for most of the properties the reported values are inconsistent. Also, when the usual predictive methods [3] are used to estimate relevant properties such as gas solubility, density or vapor pressure, large errors are obtained. Besides, group contribution methods often cannot be applied because they do not have information for the CF_2 and CF_3 groups or the information they have is not reliable, since it is based on the rare experimental data reported for perfluorocarbons. Due to the recognized limitations in the predictive models for the perfluorocarbons and the importance of these properties for the increasing practical applications, the need for precise thermophysical properties experimental data is clear.

The aim of this work is to measure the oxygen solubility, density and vapor pressure of perfluoro-*n*-octane and to develop correlative/predictive methods for the accurate estimation of these properties within the temperature and pressure range of interest. The soft-SAFT EoS has proved its capacity to describe the thermodynamic properties of pure and complex mixtures of diverse fluids. This capacity is mainly due to the theoretical background of the equation as well as to its formulation, which is straightforward to adapt according to the system in study. In this work, the soft-SAFT EoS is used to correlate liquid densities and vapor pressures measured for pure perfluoro-*n*-octane and the solubility of oxygen in perfluoro-*n*-octane.

2. Experimental

2.1. Materials

Chemicals used for the measurements were oxygen from Air Liquide with 99.999% mol/mol minimum stated purity and perfluoro-*n*-octane from Aldrich with a stated purity of 98%. Solvent and gas were used without further purification.

2.2. Density measurements

The density of perfluoro-*n*-octane was measured with a vibrating tube Antón Paar DSA-48 densimeter between 288.15 and 313.15 K at atmospheric pressure. The measuring principle is based on the calculation of the frequency of resonance of a mechanic oscillator with a given mass and volume, which is excited to be in resonance. The cell used to measure the density has a U shape and is inserted in a glass jacket filled with a high thermal conductivity gas and covered with copper in order to guarantee a proper heat transfer between the

thermostat and the measuring sample. The precision of the measurements is $\pm 5 \times 10^{-5} \text{ g cm}^{-3}$.

2.3. Vapor pressure measurements

Vapor pressures were measured using an apparatus based on the static method which consists mainly of a glass sample cell, a thermostatic water bath and a temperature and pressure measurement systems. The apparatus and the experimental method are described in more detail elsewhere [4] and here only a brief resume is given.

The experimental procedure starts with the degass of the liquid perfluoro-*n*-alkane which in this work was done through successive melting/freezing cycles while vacuum pumping non-condensable gases. The sample cell with a volume of 10 cm^3 , containing the degassed solvent is immersed in the thermostatic water bath while the system is let to evacuate. When the equilibrium temperature is reached, the apparatus is isolated from the vacuum source and the sample cell valve is opened to connect the sample container to the quartz pressure sensor. After pressure stabilization its value is recorded. Due to the purity of the sample used, three to four purge cycles are done at 333 K before starting the measurements. This procedure facilitates the removal of impurities with higher volatilities. The number of purge cycles can be increased if two consecutive vapor pressure values measured at this temperature do not originate reproducible values within the experimental error.

The temperature of the glass sample cell was measured with a calibrated Pt100 temperature sensor with an uncertainty of $\pm 0.05 \text{ K}$. The stability of the temperature in the working area of the thermostatic bath was better than $\pm 0.01 \text{ K}$. In pressure measurements, a high precision temperature compensated quartz pressure transducer was used. The accuracy of the pressure transducer is $\pm 0.01\%$ in the working range (0–1.38 MPa).

2.4. Solubility measurements

The solubility apparatus and procedure employed are similar to that described by Ben Naim and Baer [5] where the solubility is determined by measuring the quantity of gas dissolved in an accurately known volume of solvent at constant pressure and temperature. The apparatus depicted in Fig. 1 has a simple design and can be easily adapted in order to measure the solubility of systems with different solubilities. It consists mainly of a mercury manometer, M, with a mercury reservoir, R, a dissolution cell, Ve, and a gas line with a pre-saturator, PS, where the gas is saturated with the solvent.

The equilibrium cell, Ve, is based on the design of Carnicer [6] and was previously calibrated with mercury, by measuring the mercury levels in the cell capillaries and the corresponding weight of mercury. A relation between mercury levels and the cell volume is obtained being the cell volume approximately 7 cm^3 . The entire apparatus is immersed in a Perspex isolated air bath capable of maintaining the temperature to

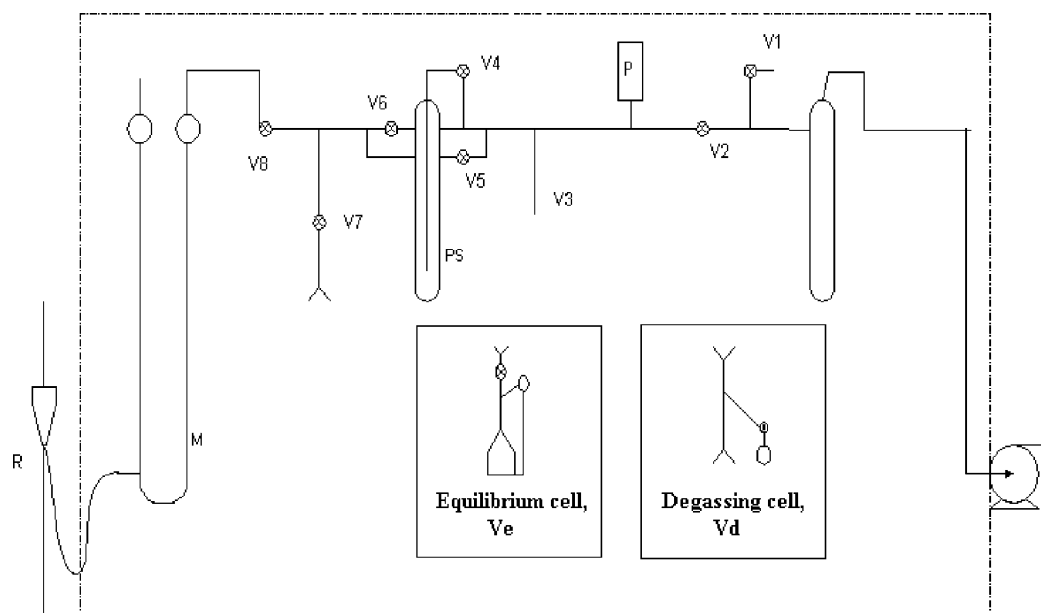


Fig. 1. Experimental apparatus: Vi, valves; PS, pre-saturator; P, vacuum gauge; M, mercury manometer; R, mercury reservoir.

within 0.1 K by means of a PID controller. The temperature is measured with a previously calibrated 25 Ω platinum resistance thermometer connected to a digital multimeter 34401 A from Agilent for temperature values acquisition.

An accurate determination of solubilities using the saturation method requires the solvent to be completely degassed. The degassing cell, Vd, filled with pure solvent is connected to the solubility apparatus. Opening valve V₁ the entire line can be connected to a vacuum source, a RV3 high vacuum pump from Edwards, capable of reaching a vacuum of 0.08 mbar. The solvent is then degassed by successive melting/freezing cycles while vacuum pumping non-condensable gases. The degassing is considered complete when no pressure variation for two consecutive cycles are detected with the pressure gauge, P. Besides being an expeditious method, the quantity of solvent lost with this degassing method is minimum when compared with other degassing procedures. By turning upside down the degassing cell, the equilibrium cell can be connected to the system and filled with the degassed solvent under its own vapor pressure.

After evacuating the system, the solute gas is introduced in the line through valve V₃. Closing valves V₂ and V₅, the gas is forced to bubble slowly in the degassed solvent contained in the saturation chamber, PS and the system is filled with the solvent-saturated gas up to a total pressure close to 1 atm. When the mercury levels in the manometer are equal, the system is isolated from the pre-saturator and is let to equilibrate. The dissolution process is initiated by turning the liquid circulation on, forcing the solvent up the right capillary arm and to circulate through the left capillary arm forming a very thin film. As gas dissolves, the system pressure is maintained at initial pressure by allowing the mercury from the reservoir to displace the gas in the system. After 15 min more then 95% of the gas is already dissolved. For perfluoro-*n*-octane

the equilibrium is reached in about half an hour. The system is considered to have reached equilibrium when no further gas is dissolved. The displacement of the mercury level was measured with a cathetometer with a precision of ± 0.01 mm. Direct reading of the mercury levels of mercury and solvent levels in the equilibrium cell are the only measurements required to calculate the volume of gas dissolved in a given volume of solvent.

2.4.1. Data reduction

There are several methods to express the solubility of a gas in a liquid. In this work, the experimental solubility results are expressed in terms of Ostwald coefficient and solute molar fraction.

The Ostwald coefficient itself can be expressed in a number of ways, although the differences between the various forms of the coefficient are negligible for low solubilities and for precisions in the solubility of 1% or poorer [7]. In this work, the Ostwald coefficient for solution volume was used. It is defined as:

$$L_{2,1}(T, p) = \left(\frac{V_g}{V_l} \right)_{\text{equil}} \quad (1)$$

where V_g is the volume of gas dissolved and V_l the total volume of the liquid solution after equilibrium is reached, at a given temperature T and pressure p . Both quantities are obtained directly from the experimental measurement.

The molar fraction of component 2 (the gaseous solute) in the liquid solution can be directly related to the Ostwald coefficient by:

$$x_2 = \frac{L_{2,1}(T, p)p_2V^L(T, p)}{Z_{12}RT} \quad (2)$$

where p_2 is the partial pressure of the solute, $V^L(T, p)$ the molar volume of the liquid solution and Z_{12} the compressibility factor of the gas estimated in this work as:

$$Z_{12} = 1 + \frac{P}{RT}(y_1 B_{11} + y_2 B_{22} + y_1 y_2 \delta_{12}) \quad (3)$$

B_{11} and B_{22} are the second virial coefficients for the pure solvent and the pure solute, respectively and $\delta_{12} = 2B_{12} - B_{11} - B_{22}$, where B_{12} is the solute-solvent cross second virial coefficient. The mole fractions in the vapor phase in equilibrium with the liquid solution, y_i , are calculated by an iterative process using the vapor–liquid equilibrium equation [8]:

$$y_1 = (1 - x_2) \left(\frac{p_1^{\text{sat}}}{p} \right) \left(\frac{\Phi_1^{\text{sat}}}{\Phi_1} \right) \exp \left[\frac{V_1^0(p - p_1^{\text{sat}})}{RT} \right] \quad (4)$$

The molar volume of the liquid solution, $V^L(T, p)$ was taken as the molar volume of the pure solvent, V_1^0 , calculated from the experimental density measurements performed in this work. The solvent's vapor pressure, p_1^{sat} , was also measured in this work. The second virial coefficient for the solute was taken from the compilation of Dymond and Smith [9] and both B_{11} and B_{12} were estimated using the correlation of Tsonopoulos [3] without any adjustable parameters.

3. Modeling

3.1. Regular Solution Theory

According to the definition of Hildebrand et al. [10], a regular solution is one involving no entropy and no volume change when a small amount of one of its components is transferred to it. Considering this assumption, the following equation can be deduced in order to describe the solubility of a non-polar gas in a non-polar solvent [10]:

$$-\log x_2 = -\log x_2^i + \frac{0.4343 \bar{V}_2}{RT} (\delta_1 - \delta_2)^2 \quad (5)$$

In this equation x_2 is the mole fraction gas solubility, x_2^i is the ideal gas solubility, \bar{V}_2 is the partial molar volume of the gas in the solution and δ_1 and δ_2 are the solubility parameters for the solvent and the solute, respectively.

When the entropic contribution is significant, the Regular Solution Theory alone cannot describe correctly the solubility of a solute in a solvent. The entropic contribution can be accounted for, if the Flory–Huggins combinatorial term is introduced:

$$-\log x_2 = -\log x_2^i + \log \frac{\bar{V}_2}{V_1} + 0.4343 \left(1 - \frac{\bar{V}_2}{V_1} \right) + \frac{0.4343 \bar{V}_2}{RT} (\delta_1 - \delta_2)^2 \quad (6)$$

where V_1 is the molar volume of the solvent.

Eq. (6) requires three parameters for the solute (x_2^i , \bar{V}_2 , δ_2) and two parameters for the solvent (V_1 and δ_1). All these parameters are temperature dependent, but the assumptions made by the Regular Solution Theory imply that the term $\bar{V}_2(\delta_1 - \delta_2)$ must be temperature independent [11]. Accordingly, any convenient temperature may be used to specify \bar{V}_2 and δ_2 , if the same temperature is used for δ_1 and V_1 . In this work, the chosen temperature was 298 K. The ideal gas solubility however, must be treated as a function of temperature. The ideal gas solubility is calculated from:

$$-\log x_2^i = \frac{\Delta H_2^{\text{vap}}}{4.575} \left(\frac{1}{T_b} - \frac{1}{T} \right) \quad (7)$$

as suggested by Gjaldbaek [12], where ΔH_2^{vap} is the solute's Enthalpy of vaporization at its boiling point T_b .

3.2. Soft-SAFT EoS

The application of the soft-SAFT equation to describe thermodynamic properties like densities and vapor pressures as well as oxygen solubility in perfluorocarbons was done before by the authors [13]. Only a brief overview is given here.

The SAFT EOS is generally formulated in terms of the residual molar Helmholtz energy, A^{res} , defined as the molar Helmholtz energy of the fluid relative to that of an ideal gas at the same temperature and density. A^{res} is written as the sum of three contributions:

$$A^{\text{res}} = A^{\text{total}} - A^{\text{ideal}} = A^{\text{ref}} + A^{\text{chain}} + A^{\text{assoc}} \quad (8)$$

A^{ref} , which accounts for the pairwise intermolecular interactions of the reference system, A^{chain} , that evaluates the free energy due to the formation of a chain from units of the reference system, and A^{assoc} , which takes into account the contribution due to site–site association. For molecules that do not associate, the association term is null. A more detailed description of each term can be found elsewhere [13].

The SAFT model describes a pure non-associating fluid as homonuclear chains composed of equal spherical segments bonded tangentially. Different fluids will have different number of segments, m , segment diameter, σ , and segment interaction energy, ε . For molecules that may associate, the association energy parameter, ε^{ij} and the association volume parameter k^{ij} are also defined to characterize the interactions between the associating sites of species i and j . When dealing with mixtures that are highly non-ideal, the Lorentz–Berthelot cross-interaction size and energy parameters need also to be adjusted to experimental data.

According to Mack and Oberhammer [14], ab initio calculations of the interaction potentials for the complex $\text{CF}_4\text{--O}_2$ provide evidence that an interaction between the oxygen and the positive carbon nucleus in CF_4 occurs, forming a very strong complex. Admitting that the same interactions can be found between oxygen and higher order perfluoroalkanes, a free energy of cross-association between oxygen and perfluoroalkane molecules was considered. Consequently, both

Table 1
Experimental and calculated liquid densities of perfluoro-*n*-octane

T (K)	ρ_{exp} (g cm ⁻³)	Power series equation ρ_{calc} (g cm ⁻³)	$\delta\rho^a$ (g cm ⁻³)	Soft-SAFT EoS ρ_{calc} (g cm ⁻³)	$\delta\rho^a$ (g cm ⁻³)
288.15	1.79015	1.79005	0.00009	1.78082	0.00932
293.15	1.77749	1.77751	-0.00002	1.76827	0.00922
298.15	1.76475	1.76481	-0.00006	1.75559	0.00916
303.15	1.75187	1.75195	-0.00008	1.74279	0.00908
313.15	1.72579	1.72572	0.00007	1.71682	0.00897

$$^a \delta\rho = \rho_{\text{exp}} - \rho_{\text{calc}}$$

molecular oxygen and perfluoroalkanes were modeled as associating molecules with two association sites on each.

Molecular parameters of the non-associating model for the pure compounds were estimated by fitting vapor pressures and saturated liquid densities to the experimental data measured in this work. In the case of the oxygen/perfluoro-*n*-octane mixture, the binary size and energy interaction parameters were fitted to experimental solubility data as well as the two cross-association parameters.

4. Results and discussion

4.1. Density

Experimental density values obtained in this work are presented in Table 1 and were fitted to a power series of the type suggested by Steele et al. [15]:

$$\rho_{\text{calc}} = \rho_c + \sum_{i=1}^2 A_i (1 - T_r)^{i/3} \quad (9)$$

where ρ_c is the critical density and T_r is the reduced temperature. The critical constants T_c and ρ_c were obtained from Vandana et al. [16] and are equal to 498.5 K and 0.6109 g cm⁻³, respectively.

The values obtained for the coefficients in Eq. (9) are $A_1 = 1.04566$ and $A_2 = 0.70186$ describe liquid densities of perfluoro-*n*-octane with an absolute average deviation (AAD) of 0.004%. The density values reported by Kreglewski [17] and Haszeldine [18] are compared in Fig. 2 with the data measured in this work. These authors do not state the purity of their compounds and measured densities with pycnometers. The values obtained in this work agree well with the ones measured by Kreglewski [17] but differ to within 0.7% from the ones given by Haszeldine [18]. This deviation is probably due to differences in the purities of the compounds used.

Table 1 also presents the values calculated with the soft-SAFT EoS. The molecular parameters m , σ and ε/κ_B for perfluoro-*n*-octane are equal to 3.522, 4.521 Å and 245.1 K, respectively. Using these parameters, liquid densities were fitted with an AAD lower than 0.2 %.

4.2. Vapor pressure

Experimental vapor pressure data are listed in Table 2 and were fitted to the Antoine equation:

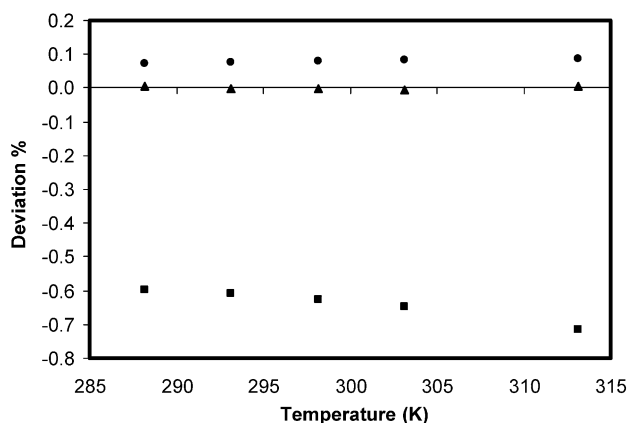


Fig. 2. Comparison between correlated experimental liquid density data measured in this and experimental data measured in this work (▲) and literature data measured by Kreglewski [17] (●) and Haszeldine [18] (■) for perfluoro-*n*-octane. Deviation is defined as $(\rho_{\text{exp}} - \rho_{\text{lit}})/\rho_{\text{lit}} \times 100$.

$$\ln \left(\frac{P}{\text{kPa}} \right) = A - \frac{B}{(T/\text{K}) + C} \quad (10)$$

The Antoine constants adjusted to the experimental data are $A = 18.921$, $B = 5892.038$ and $C = 36.717$ describe the vapor pressures of perfluoro-*n*-octane with an AAD equal to 0.5%.

The obtained data are compared with the only data found in the open literature for perfluoro-*n*-octane [17] in Fig. 3.

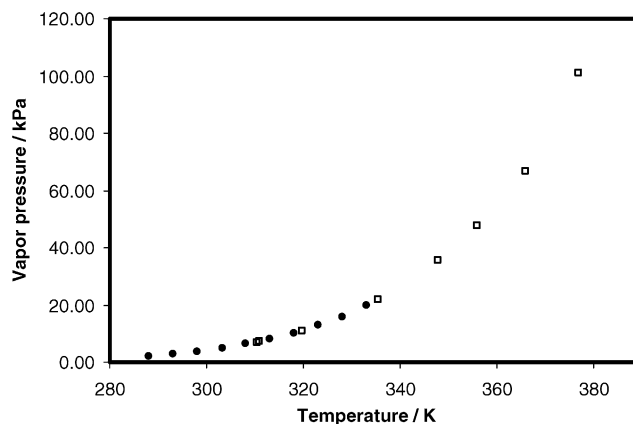


Fig. 3. Comparison between experimental vapor pressure data measured in this work (●) and experimental data measured by Kreglewski [17] (□) for perfluoro-*n*-octane.

Table 2
Experimental and calculated vapor pressure, normal boiling point and enthalpy of vaporization, of perfluoro-*n*-octane

T (K)	P_{exp} (kPa)	Antoine's equation P_{calc} (kPa)	δP^a (kPa)	Soft-SAFT EoS P_{calc} (kPa)	δP^a (kPa)
288.13	2.21	2.19	0.02	1.98	0.23
293.03	2.85	2.87	-0.01	3.03	-0.17
298.14	3.74	3.76	-0.03	4.15	-0.41
303.34	4.88	4.93	-0.04	5.39	-0.51
308.19	6.32	6.29	0.04	6.72	-0.39
313.09	8.02	7.99	0.04	8.28	-0.26
318.17	10.19	10.16	0.02	10.21	-0.03
323.14	12.86	12.78	0.08	12.48	0.38
328.15	15.96	16.00	-0.05	15.22	0.74
333.21	19.89	19.96	-0.07	18.50	1.38
ΔH^{vap} ($T = 298.15$ K) (kJ mol ⁻¹)			39.88		
T_b (K)			375.23		

$$^a \delta P = P_{\text{exp}} - P_{\text{calc}}$$

Table 3
Results obtained for the solubility of oxygen in *n*-heptane

T (K)	$L_{2,1}(T, p)$ (%)			
	This work	Hesse et al. (1996) [19]	Makranczy et al. (1976) [20]	Thomsen and Gjaldbaek (1963) [21]
298.15	0.335 ± 1	0.338 ± 0.5	0.322 ± 3	0.330 ± 1
299.24	0.325 ± 1			
303.00	0.307 ± 1			
303.15	0.306 ± 1			

The values obtained in this work are 2% lower than the values measured by Kreglewski [17] and the Antoine's equation parameters proposed by the author cannot describe the vapor pressure data for temperatures below 310.47 K.

Also in Table 2, the vapor pressure values obtained with the soft-SAFT EoS using the molecular parameters given in Section 4.1 are reported. The equation fits the experimental data with an AAD of about 4%.

Values for the Enthalpy of vaporization and the boiling point were calculated from the vapor pressure data by means of the Clapeyron equation assuming that the vapors behave as an ideal gas. Both values are also presented in Table 2.

4.3. Oxygen solubility

To estimate the precision of the experimental apparatus, the solubility of oxygen in *n*-heptane was measured and compared with literature values in Table 3. The result obtained at 298 K deviates 0.8%, 4.0% and 1.5% from the values reported by Hesse et al. [19], Makranczy et al. [20] and Thomsen and Gjaldbaek [21], respectively. Our value agrees with the experimental data measured by these authors within the experimental error reported by them. Also, the precision of this method is well described by the good agreement of the values obtained at 303.00 and 303.15 K.

Table 4 shows the experimental values obtained for the solubility of oxygen in perfluoro-*n*-octane between 288 and 313 K and pressures close to atmospheric. The temperature dependence of the experimental values of the solubilities

expressed in mole fraction $x_2(T, p)$, was correlated using the following equation suggested by Benson and Krause [22]:

$$\ln x_2 = \sum_{i=0}^2 A_i T^{-i} \quad (11)$$

The values obtained for the coefficients were $A_1 = -6.908 \times 10^1$, $A_2 = 3.691 \times 10^4$, $A_3 = -5.338 \times 10^6$. The AAD of the experimental results obtained for the solubility of the oxygen in perfluoro-*n*-octane is 0.70%.

4.3.1. Thermodynamic functions

The dissolution of a gas into a liquid is associated with changes in thermodynamic functions namely standard Gibbs energy (ΔG_2^0), standard enthalpy (ΔH_2^0) and standard entropy (ΔS_2^0) of solution that can be calculated from

Table 4
Experimental data for the solubility of oxygen in perfluoro-*n*-octane between 288 and 313 K expressed as Ostwald's coefficients and solute mole fraction, at the partial pressure of the gas, p_2

T (K)	p_2 (MPa)	$L_{2,1}(T, p)$	$10^3 x_2$
290.0	0.0990	0.510 ± 0.004	5.14 ± 0.04
292.0	0.0992	0.512 ± 0.004	5.15 ± 0.04
297.1	0.0976	0.503 ± 0.004	4.92 ± 0.04
299.9	0.0962	0.487 ± 0.004	4.67 ± 0.03
304.5	0.0960	0.465 ± 0.003	4.42 ± 0.03
308.7	0.0943	0.436 ± 0.003	4.04 ± 0.03
313.1	0.0937	0.386 ± 0.003	3.53 ± 0.03

Table 5
Thermodynamic properties of solution for oxygen in perfluoro-*n*-octane

T (K)	ΔG_2^0 (kJ mol ⁻¹)	ΔH_2^0 (kJ mol ⁻¹)	ΔS_2^0 (J mol ⁻¹ K ⁻¹)
290.0	12.7	1.1	-39.9
292.0	12.7	-1.0	-47.1
297.1	13.0	-6.2	-64.6
299.9	13.2	-8.9	-73.9
304.5	13.6	-13.4	-88.8
308.7	14.0	-17.4	-101.6
313.1	14.5	-21.5	-114.7

experimental solubility results. These functions represent the changes that occur in the solute neighborhood during dissolution process due to the transference of one solute particle from the pure perfect gas state to an infinitely dilute state in the solvent, at a given temperature T [23]. The thermodynamic functions were calculated from the temperature dependence of the molar fraction according to the following equations [24]:

$$\Delta G_2^0 = -RT(\ln x_2)_p \quad (12)$$

$$\Delta H_2^0 = RT^2 \left(\frac{\partial(\ln x_2)}{\partial T} \right)_p \quad (13)$$

$$\Delta S_2^0 = R \left(\frac{\partial(\ln x_2)}{\partial(\ln T)} \right)_p \quad (14)$$

where R is the gas constant.

The values for the thermodynamic functions of solution of oxygen in perfluoro-*n*-octane are listed in Table 5. These results were obtained considering the ideal gas state at 101,325 Pa. No data obtained by calorimetric measurements were found for comparison. Both negative enthalpies and entropies of solution are in agreement with the decrease of the solute's solubility with the temperature. As discussed by Prausnitz et al. [8], negative entropies of solution appear when relatively large gas solubilities take place and the negative enthalpy of mixing is connected to the small difference in cohesive energy densities between the solute and the solvent is small, which is the case for the system in study.

4.3.2. Modeling solubility data

The large entropic contribution for the solubility of oxygen in perfluoro-*n*-octane justifies the use of a Flory Huggins term coupled to the Regular Solution Theory in Eq. (6) to predict the solubility data.

The partial molar volume of the gas, \bar{V}_2 , and the solubility parameter of the solute, δ_2 , were obtained from Prausnitz and Shair [11] and are equal to 33.0 cm³ mol⁻¹ and 16.7 (J cm⁻³)^{1/2}, respectively.

The ideal gas solubility is calculated from Eq. (7) using an oxygen's Enthalpy of vaporization, ΔH_2^{vap} , equal to 6785.1 J mol⁻¹ [25] at its boiling point T_b , 90.188 K [25].

The solvent's parameters are the molar volume, V_1^0 , taken from this work at 298 K, and the solubility parameter of the

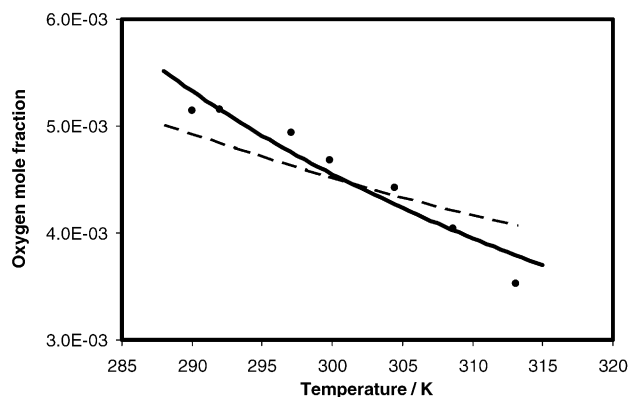


Fig. 4. Comparison between experimental results (●) and calculated values given by the Regular Solution Theory (dashed line), and by the soft-SAFT EoS (solid line) for the solubility of oxygen in perfluoro-*n*-octane in the temperature range of 288 and 313 K.

solvent, δ_1 is defined as:

$$\delta_1 = \sqrt{\frac{\Delta H_1^{\text{vap}} - RT}{V_1^0}} \quad (15)$$

The solvent's Enthalpy of vaporization ΔH_1^{vap} , was calculated from the temperature dependence of the vapor pressure measured and is given in Table 2. Using the Clausius–Clapeyron equation, ΔH_1^{vap} was calculated at a mean temperature equal to 310.50 K and then corrected to a reference temperature, in this case equal to 298.15 K, using the correlation mentioned by Chickos [26]. The calculated value of δ_1 is equal to 12.3 (J cm⁻³)^{1/2} which agrees well with the value reported by Hildebrand et al. [10] for similar perfluorocarbons.

A comparison between the experimental data and the predictions obtained by the Regular Solution Theory is presented in Fig. 4. The proposed model based on the Regular Solution Theory can provide a reasonable description of the oxygen solubility in perfluoro-*n*-octane with an AAD of 6% in the temperature range studied. Note that the model cannot correctly describe the temperature dependence of the solubility data.

The solubility data was also correlated with the soft-SAFT EoS. Binary interaction size and energy parameters were fitted to experimental solubility data, and they are equal to 1.599 and 1.044, respectively. The magnitude of the site–site interaction between oxygen and perfluoroalkane molecules in the SAFT model depends on the two cross-association parameters, $\varepsilon^{ij} = 2000$ K and $k^{ij} = 8000$ Å³. These values provide the proper solubility dependence with temperature, which was impossible to reproduce without the association contribution. The description of the solubility of oxygen in perfluoro-*n*-octane by soft-SAFT EOS is shown in Fig. 4 as a solid line. As can be observed, the main advantage of the soft-SAFT model including cross-association when compared with the Regular Solution Theory is that it reproduces more accurately the temperature dependence of oxygen solubility in perfluoro-*n*-octane.

Table 6

Comparison between the properties required to a perfluorocarbon liquid to be used intravenously and the properties shown by perfluoro-*n*-octane

	Required properties of a liquid to be used intravenously [2]	Properties of C ₈ F ₁₈
Molecular weight	420 ≤ MW ≤ 460	438.06
Density (g cm ⁻³) at 298.15 K	≤2.0	1.76 ^a
Surface tension (mN m ⁻¹) at 298.15 K	≤17	13.55 [27]
Viscosity (cP) at 298.15 K	≤5	1.93 [18]
Vapor pressure (kPa) at 298.15 K	≤13	3.74*
Boiling point (K)	≥328	375.23*
O ₂ solubility at 310 K, (ml O ₂ /ml solution)	High	0.42*

^a This work.

5. Conclusions

Liquid densities, vapor pressures and oxygen's solubility in perfluoro-*n*-octane were accurately measured in this work. Original solubility data is presented and a comparison with literature data was done for liquid density and vapor pressure data.

The measurement of the mentioned properties is important to investigate the capacity of perfluoro-*n*-octane to be used intravenously for medical applications. As shown in Table 6, perfluoro-*n*-octane fulfills the most important conditions required for such application.

New parameters for the description of perfluoro-*n*-octane using the soft-SAFT EoS are proposed. The soft-SAFT EoS was used to correlate the experimental data within 0.2, 4.3 and 4.0% for liquid density, vapor pressure and oxygen solubility, respectively. With respect to the oxygen solubility in perfluoro-*n*-octane, the soft-SAFT equation demonstrated to describe more properly the accentuated temperature dependence of the experimental data when compared with the Regular Solution Theory.

List of symbols

B	second virial coefficient (m ³ mol ⁻¹)
p	pressure (MPa)
R	universal gas constant (8.314 × 10 ⁻³ Pa m ³ mol ⁻¹ K ⁻¹)
T	temperature (K)
V	volume (m ³)
\bar{V}	partial molar volume (cm ³ mol ⁻¹)
x	mole fraction of the solute in the liquid phase
y	mole fraction of the solute in the gaseous phase
Z	compressibility factor
ΔG^0	standard Gibbs energy (kJ mol ⁻¹)
ΔH^0	standard enthalpy of solution (kJ mol ⁻¹)

ΔS^0 standard entropy of solution (J mol⁻¹ K)
 ΔH^{vap} enthalpy of vaporization (J mol⁻¹)

Greek letters

ϕ fugacity coefficient
 δ solubility parameter (J cm⁻³)^{1/2}
 ρ density (g cm⁻³)

Subscripts

1 solvent
 2 solute
 b boiling
 c critical
 calc calculated
 exp experimental
 g dissolved gas
 l liquid solution in equilibrium
 r reduced property

Superscript

0 pure component
 i ideal
 L liquid solution
 sat saturated property

Acknowledgements

This project was financed by Fundação para a Ciência e Tecnologia, POCTI/35435/EQU/2000. A.M.A. Dias is grateful to Fundação para a Ciência e Tecnologia for the Ph.D. grant SFRH/BD/5390/2001.

References

- [1] J. Riess, Chem. Rev. 101 (2001) 2797–2920.
- [2] J. Riess, Fluorocarbon-based oxygen-delivery: basic principles and product development, in: T. Chang (Ed.), Blood Substitutes: Principles, Methods, Products and Clinical Trials, vol. 2, Karger Landes Systems, Switzerland, 1998.
- [3] B. Poling, J. Prauznitz, J. O'Connell, The properties of Gases and Liquids, fifth ed., McGraw-Hill, New York, 2001.
- [4] A.I. Caço, A.M.A. Dias, L.M.N.B.F. Santos, M.M. Piñeiro, L.F. Vega, J.A.P. Coutinho, I.M. Marrucho, unpublished results.
- [5] A. Ben Naim, R. Battino, J. Solution Chem. 14 (1985) 245–253.
- [6] J. Carnicer, F. Gibanel, J. Urieta, C. Losa, Rev. Acad. Ciencias Zaragoza 34 (1979) 115–119.
- [7] R. Battino, Fluid Phase Equilibr. 15 (1984) 231–240.
- [8] J. Prausnitz, R. Lichtenthaler, E. Azevedo, Molecular Thermodynamics of Fluid-Phase Equilibria, third ed., Prentice Hall, New Jersey, 1999.
- [9] J. Dymond, E. Smith, The Virial Coefficients of Pure Gases and Mixtures, Oxford University Press, Oxford, 1980.
- [10] J. Hildebrand, J. Prausnitz, R. Scott, Regular Related Solutions—The solubility of Gases, Liquids and Solids, Van Nostrand Reinhold, New York, 1970.
- [11] J. Prausnitz, F. Shair, A.I.Ch.E. J. 7 (4) (1961) 682–687.
- [12] J. Gjaldbaek, Acta Chemica Scandinavica 6 (1952) 623–633.

- [13] A.I. Caço, J.C. Pàmies, J.A.P. Coutinho, I.M. Marrucho, L.F. Vega, *J. Phys. Chem. B* 108 (2004) 1450–1457.
- [14] H.G. Mack, H.J. Oberhammer, *J. Chem. Phys.* (1987) 87.
- [15] W. Steele, R. Chirico, S. Knipmeyer, A. Nguyen, *J. Chem. Eng. Data* 42 (1997) 1021–1036.
- [16] V. Vandana, D. Rosenthal, A. Teja, *Fluid Phase Equilib.* 99 (1994) 209–218.
- [17] A. Kreglewski, *Bulletin de L'academie Polonaise des Sciences X* (1962) 629–631.
- [18] R. Haszeldine, F. Smith, *J. Chem. Soc.* (1951) 603–608.
- [19] P. Hesse, R. Battino, P. Scharlin, E. Wilhelm, *J. Chem. Eng. Data* 41 (1996) 195–201.
- [20] J. Makranczy, et al., *Hungarian J. Ind. Chem.* 4 (1976) 269–279.
- [21] E. Thomsen, J. Gjaldbaek, *Acta Chemica Scandinavica* 17 (1963) 127–133.
- [22] B. Benson, D. Krause, *J. Chem. Phys.* 64 (1976) 689–709.
- [23] A. Ben Naim, *Hydrophobic Interactions*, Plenum Press, New York, 1980.
- [24] E. Wilhelm, R. Battino, R. Wilcock, *Chem. Rev.* 77 (2) (1977) 219–262.
- [25] DIPPR, *Thermophysical Properties Database*, 1998.
- [26] J.S. Chickos, *J. Org. Chem.* 57 (1992) 1897–1899.
- [27] A.I. Caço, A.M.A. Dias, J.A.P. Coutinho, I.M. Marrucho, unpublished results.